

ditions," AIAA Paper 91-75, 1991.

¹⁰Yang, V., Lin, N. N., and Shuen, J. S., "Vaporization of Liquid Oxygen (LOX) Droplets at Supercritical Conditions," AIAA Paper 92-103, 1992.

¹¹Chiu, H. H., and Gross, K. W., "Liquid Behavior at Critical and Supercritical Conditions," JANNAP Workshop Summary, Irvine, CA, 1986.

¹²Yang, A. S., Hsieh, W. H., Kuo, K. K., and Brown, J. J., "Evaporation of LOX Under Supercritical and Subcritical Conditions," AIAA Paper 93-2188, 1993.

¹³Yang, A. S., "Combustion of LOX with H₂(g) Under Subcritical and Supercritical Conditions," Ph.D. Dissertation, Pennsylvania State Univ., University Park, PA, 1993.

¹⁴Sychev, V. V., Vasserman, A. A., Kozlov, A. D., Spiridonov, G. A., and Tsyman, V. A., *Property Data Update, Official Standards of The National Standard Reference Data Service of the USSR*, Hemisphere, Washington, DC, 1987.

¹⁵Lucas, K., "Review of Present Status of Transport Properties Predictions," *Phase Equilibria and Fluid Properties in the Chemical Industry*, Dechema, Frankfurt, Germany, 1980, pp. 573-587.

¹⁶Laesecke, A., Krauss, R., and Stephan, K., "Transport Properties of Fluid Oxygen," *Journal of Physical and Chemical Reference Data*, Vol. 19, No. 5, 1990, pp. 1089-1121.

¹⁷Chapman, S., and Cowling, T. G., *The Mathematical Theory of Non-Uniform Gases*, Cambridge Univ. Press, New York, 1961.

¹⁸Takahashi, S., "Preparation of a Generalized Chart for the Diffusion Coefficients of Gases at High Pressures," *Journal of Chemical Engineering of Japan*, Vol. 7, No. 6, 1974, pp. 417-420.

¹⁹Wilke, C. R., "Diffusional Properties of Multicomponent Gases," *Chemical Engineering Progress*, Vol. 46, No. 2, 1950, pp. 95-104.

²⁰Daubert, T. E., and Danner, R. P., *Physical and Thermodynamic Properties of Pure Chemicals: Data Compilation*, Hemisphere, New York, 1989.

²¹McBride, B. J., and Zeleznik, F. J., "Computer Program for Calculation of Complex Chemical Equilibrium Compositions and Applications: Supplement I—Transport Properties," NASA TM-86885, 1984.

²²Kuo, K. K., *Principles of Combustion*, Wiley, New York, 1986.

²³Prausnitz, J. M., Lichtenthaler, R. N., and de Azevedo, E. G., *Molecular Thermodynamics of Fluid-Phase Equilibria*, Prentice-Hall, Englewood Cliffs, NJ, 1986.

²⁴Patankar, S. V., *Numerical Heat Transfer and Fluid Flows*, Hemisphere, New York, 1980.

Flow Characteristics of a Rectangular Multielement Supersonic Mixer-Ejector

R. Taghavi*

University of Kansas, Lawrence, Kansas 66045

and

G. Raman†

NYMA, Inc., Brook Park, Ohio 44142

Introduction

ONE promising method of supersonic jet noise reduction is the use of a mixer-ejector nozzle.¹⁻⁶ The work described in this Note is a part of an ongoing experimental study on the flow physics and performance characteristics of a rec-

tangular multielement supersonic mixer-ejector nozzle. The ejector characteristics studied included the mean flow at the ejector exit, ejector pumping, and the ejector sidewall static pressure. To our knowledge, the only other published work on rectangular supersonic multijet ejectors is that by Chandrasekhara et al.⁷ Their results showed that the performance of a multijet ejector is distinctly superior to that of a single equivalent jet ejector. Our main objective is to characterize the performance of multijet ejectors at various primary jet Mach numbers and area ratios (ejector area/primary jet area).

Experimental Setup and Instrumentation

A schematic diagram of the flow facility used in our experiments is shown in Fig. 1. The facility was previously described in detail in Refs. 8 and 9, therefore, only a brief description is given here. The primary jets emerged from four convergent-rectangular nozzles (6.9×34.5 mm) into the straight adjustable-area rectangular ejector. The internozzle spacing (center-to-center) was 6.25 times the narrow dimension of the nozzle. The individual nozzle total pressures were maintained to within ± 0.1 psi using an automatic feedback control loop.

The adjustable-area ejector was constructed from Plexiglas® side walls. The leading edges and spacers were made from wood. The total length of the ejector sidewall, in the streamwise direction, was 32.51 cm, which included 5.08 cm of leading edge and 4.45 cm of tapered trailing edge (only the outside surface was tapered). The small dimension of the rectangular ejector could be adjusted by the addition or removal of spacers. The large dimension could be adjusted by loosening the clamps and sliding the small sides (stack of spacers) in or out. The ejector aspect ratio, defined as the ratio of the large to small dimensions of the ejector exit, was kept constant at 4.5 for the two cases studied.

An extra sidewall was fabricated and instrumented with 121 static taps (11×11 matrix) connected to the electronic scanning pressure (ESP) modules for instantaneous mapping of the ejector sidewall static pressure distribution. The pressure tap matrix extended from the leading edge to 5.72 cm upstream of the trailing edge. The flow total pressure at the ejector exit was mapped using a pitot probe having an o.d. of 0.8 mm. The probe was traversed over the entire flowfield under computer control.

Results and Discussion

Mean Flowfield at the Ejector Exit

Mach number contours at the ejector exit plane, for two ejector area ratios ($AR = 7$ and 12) at six primary-jet fully expanded Mach numbers are shown in Fig. 2. The ejector area ratio is defined as the ratio of ejector exit area to the total exit area of the four rectangular nozzles. In these plots, the y and z coordinates are normalized by the primary nozzles' equivalent diameter D_{eq} , defined as the diameter of the circle having an area equal to the total exit area of the four primary rectangular nozzles. From the contour plots of Fig. 2 it is clear that for all primary jet Mach numbers, an increase in the ejector area ratio from 7 to 12 resulted in a reduction in the peak ejector exit Mach number and a more uniform mixing of the primary jets and secondary (ejector entrained) flow.

The ejector pumping per unit secondary area for various cases is plotted in Fig. 3. The pumping was obtained as follows. First the total mass flow at the ejector exit was calculated by integration of the data shown in Fig. 2, then the primary jet's mass flow was subtracted from the total mass flow. Finally the pumping per unit secondary area was calculated. The secondary area is the ejector exit area (constant for an ejector with parallel sidewalls) minus the total exit area of the four primary nozzles. From the plots of Fig. 3 it is clear that, for both area ratios, the ejector pumping per unit secondary area increases when the primary jet Mach number increases. For the case of $AR = 7$, the variation is almost linear, but the slope decreases as the primary jet Mach number increases beyond

Received April 21, 1995; presented as Paper 95-017 at the AIAA/CEAS 1st Joint Aeroacoustics Conference, Munich, Germany, June 12-15, 1995; revision received Feb. 23, 1996; accepted for publication March 1, 1996. Copyright © 1996 by the American Institute of Aeronautics and Astronautics, Inc. All rights reserved.

*Associate Professor, Department of Aerospace Engineering. Senior Member AIAA.

†Senior Research Engineer, NASA Lewis Research Center Group, Experimental Fluid Dynamics Section. Member AIAA.

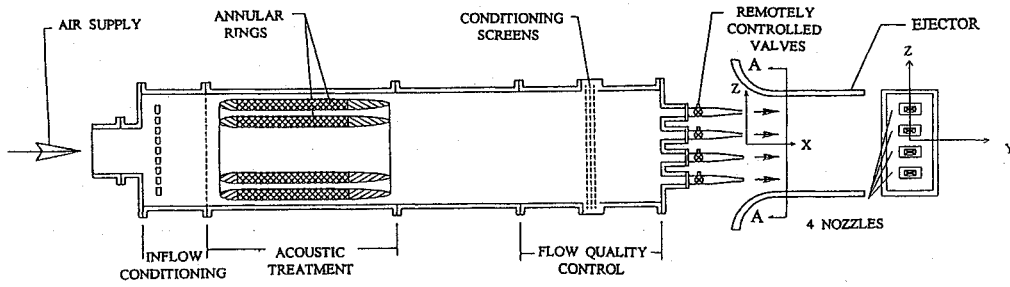


Fig. 1 Schematic of the supersonic jet flow facility.

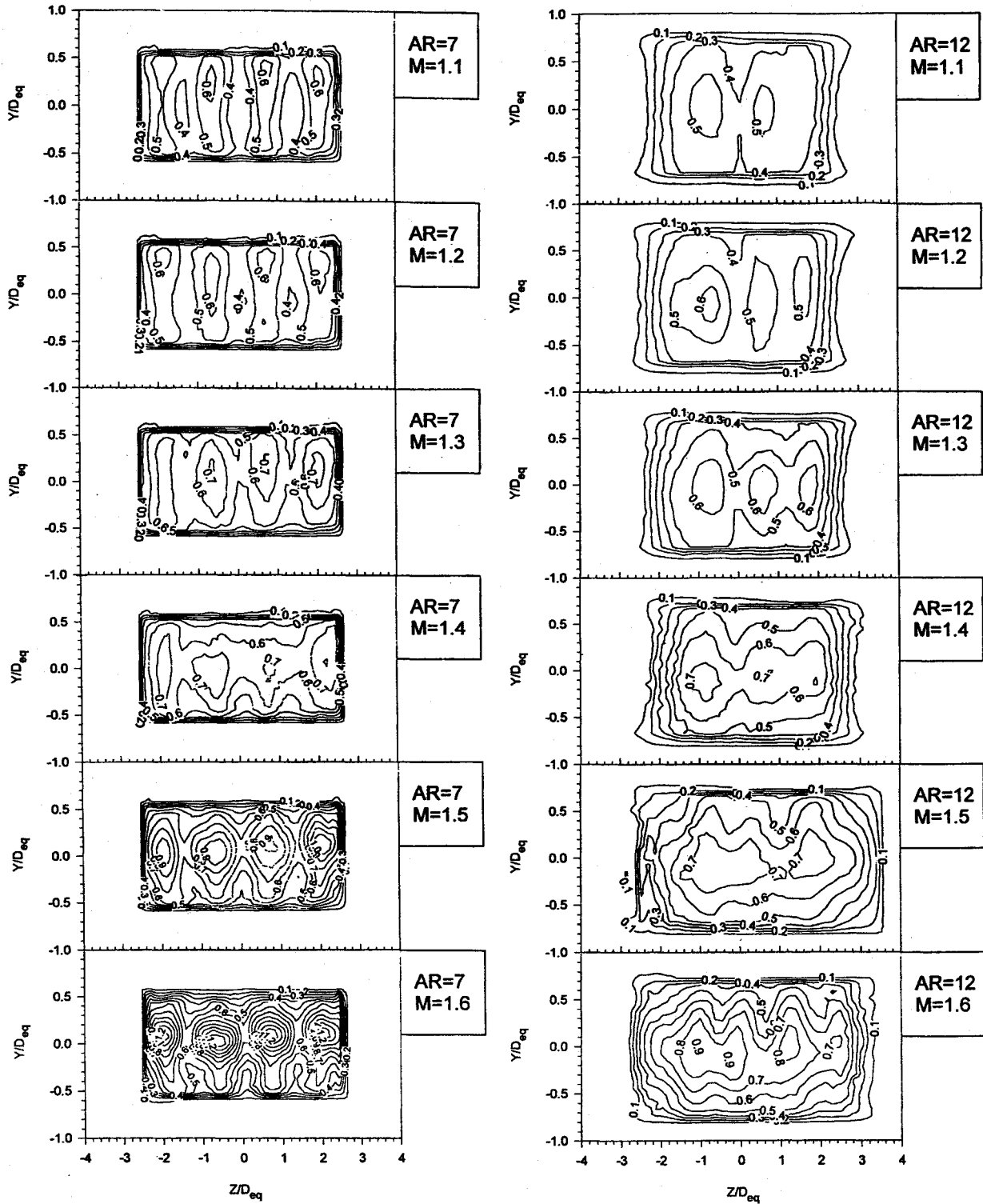


Fig. 2 Mach number contours at the ejector exit; contour interval is 0.1.

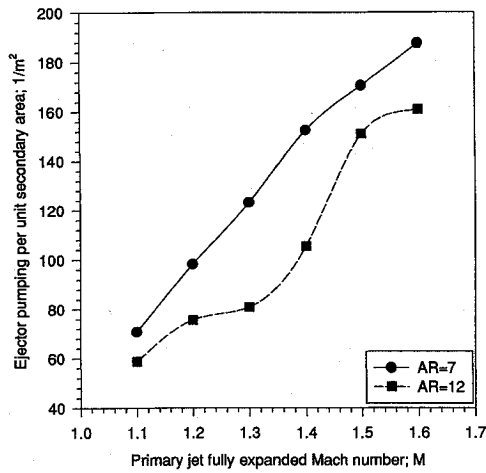


Fig. 3 Variation of ejector pumping per unit secondary area with primary jet fully expanded Mach number.

$M = 1.4$. For the case of $AR = 12$, the variation is not linear and has a very high positive slope at Mach numbers between $M = 1.3-1.5$. At all Mach numbers investigated, the ejector pumping per unit secondary area decreases when the area ratio increases from 7 to 12.

Ejector Sidewall Static Pressure Distributions

Figure 4 shows the static pressure distributions along the centerline of the ejector sidewall at different primary-jet Mach numbers and ejector area ratios. The abscissa represents the downstream distance, from the ejector leading edge, along the centerline of the ejector sidewall normalized by the primary-nozzle D_{eq} . The ordinate represents the pressure coefficient defined as $C_p = (P - P_a)/P_a$, in which P_a is ambient pressure and P is the ejector-sidewall static pressure. The ejector-sidewall static pressure indicates mixing of the primary jets and the secondary flow induced by the ejector. When the static pressure approaches the ambient value at the ejector exit, we can infer that the primary and secondary flows have mixed. The last row of the static pressure ports was located 5.72 cm

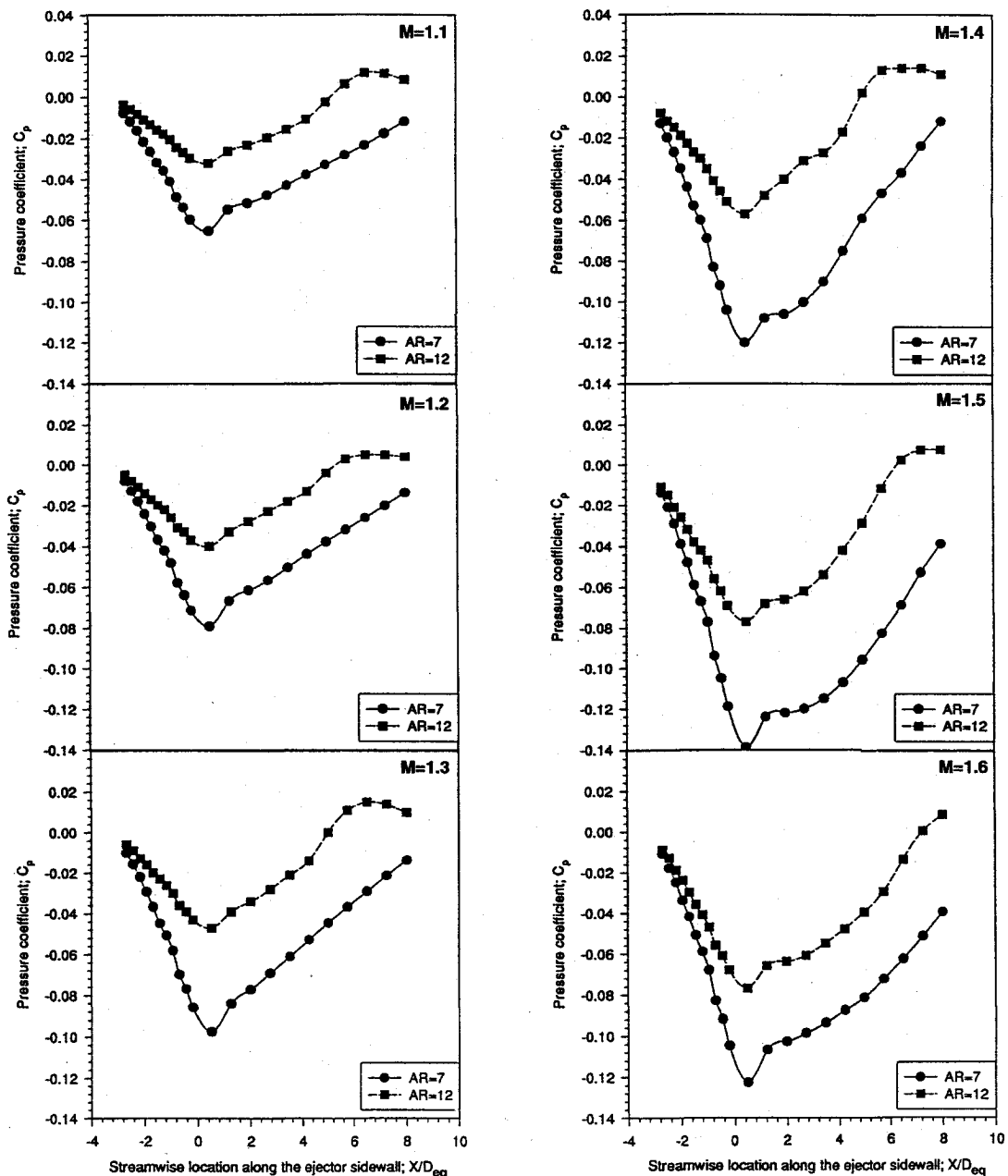


Fig. 4 Static pressure distribution along the centerline of the ejector sidewall.

upstream of the ejector exit, so the pressures indicated by this row are not the same as the ejector exit plane static pressure. Data in Fig. 4 reveal that for all Mach numbers, changing the area ratio from 7 to 12 produces a large increase in the ejector-sidewall static pressures. The case of the $AR = 12$ provides interesting results. The ejector-sidewall static pressures for this case reach the ambient value well upstream of the ejector exit. Although it may appear that for this case an ejector that is 30% shorter would function just as well, we urge caution in making such inferences. This is because a shorter ejector would comprise a different system with differing rates of pumping, mixing, and fluid-acoustic interactions.

Concluding Remarks

We present a unique set of data on the performance characteristics of a rectangular multijet mixer ejector for two ejector area ratios (7 and 12) over a range of operating conditions. The peak velocity at the ejector exit reduced when the ejector area ratio was increased from 7 to 12. Although the total pumping increased in going from $AR = 7$ to 12, the pumping per unit secondary area decreased. The previous observation was true at all Mach numbers from 1.1 to 1.6. The ejector wall static pressure that is also an indicator of pumping was always lower for the $AR = 7$ case as compared to the $AR = 12$ case.

Acknowledgments

This research was conducted under Grant NCC-251 from NASA Lewis Research Center. The authors thank John Abbott

and Khairul Zaman of NASA Lewis Research Center for their support and technical input. In addition, the authors thank Edward J. Rice for the ejector design. The efforts of Jim Nichols (mechanical), Richard Brokopp (operations), and James Little (electronics) are highly appreciated.

References

- ¹Hsia, Y.-C., Krothapalli, A., and Baganoff, D., "Mixing of an Underexpanded Rectangular Jet Ejector," *Journal of Propulsion and Power*, Vol. 4, No. 3, 1988, pp. 256–262.
- ²Bernardo, A. B., and Gutmark, E., "Rectangular Supersonic Ejector," AIAA Paper 94-2942, June 1994.
- ³Kinzie, K. W., Martens, S., and McLaughlin, D. K., "Supersonic Elliptic Jet Noise: Experiments With and Without an Ejector Shroud," AIAA Paper 93-4349, Oct. 1993.
- ⁴Lord, W. K., Jones, C. W., Stern, A. M., Head, V. L., and Krejsa, E. A., "Mixer Ejector Nozzle for Jet Noise Suppression," AIAA Paper 90-1909, July 1990.
- ⁵Tillman, T. G., and Presz, W. M., "Thrust Characteristics of a Supersonic Mixer Ejector," AIAA Paper 93-4345, Oct. 1993.
- ⁶Ahuja, K. K., "Mixing Enhancement and Jet Noise Reduction through Tabs Plus Ejectors," AIAA Paper 93-4347, Oct. 1993.
- ⁷Chandrasekhara, M. S., Krothapalli, A., and Baganoff, D., "Mixing Characteristics of an Underexpanded Multiple Jet Ejector," Stanford Univ., JIAA TR-55, Stanford, CA, 1984.
- ⁸Taghavi, R., and Raman, G., "Enhanced Mixing of Multiple Supersonic Rectangular Jets by Synchronized Screech," *AIAA Journal*, Vol. 32, No. 12, 1994, pp. 2477–2480.
- ⁹Raman, G., and Taghavi, R., "Resonant Interaction of a Linear Array of Supersonic Rectangular Jets," *Journal of Fluid Mechanics*, Vol. 309, 1996, pp. 93–111.